

## Model of the microstrip line with a non-uniform dielectric

V. Urbanavičius, R. Martavičius

Department of Electronic Systems, Vilnius Gediminas Technical University,  
Naugarduko str. 41-422, LT-03227 Vilnius, Lithuania, phone. +370 5 2744756, e. mail: vytautas.urbanavicius@el.vtu.lt

### Introduction

Microstrip lines (MSL) are broadly used in various microwave devices. Designing microwave devices it is necessary to match characteristic impedances of their separate elements. For calculations of the characteristic impedance and other MSL parameters the set of methods differing by accuracy, application conditions, requirements to computing resources, etc. is developed [1, 2].

Previously, while resources of computer were limited, electrodynamic tasks were solved by analytical methods, making calculations as small as possible. For example, calculating the characteristic impedance of the transmission lines method of conformal transformations [3], method of partial capacities [4], the integrated equations method [5], and spectral-domain method [6] were applied. Now it is more preferable to use more ordinary methods, but not paying attention to requirements to computing resources, for example finite-difference method [7, 8], method of moments [9], artificial neural networks [10], etc.

In this paper, using the method of moments [11] the mathematical model of MSL with the non-uniform dielectric is created, and the results of its analysis are represented.

### Principles of mathematical model of the microstrip line

The method of moments allows to find distribution of the electric charge density of MSL in uniform dielectric according to potentials on conducting surfaces [12]. However the MSL with non-uniform dielectric more often are used. The generalized structure of such a line is shown in Fig. 1. In this line the signal strip is placed on the surface of the dielectric substrate above which an air there is, and because of that the dielectric environment in cross-section of the line becomes non-uniform.

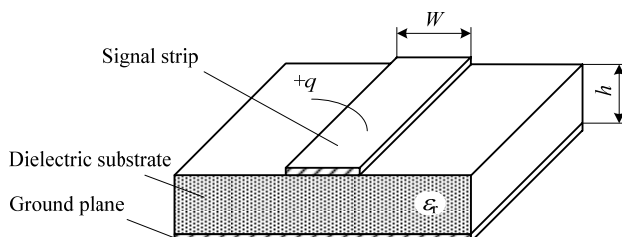


Fig. 1. The geometry of the microstrip line.

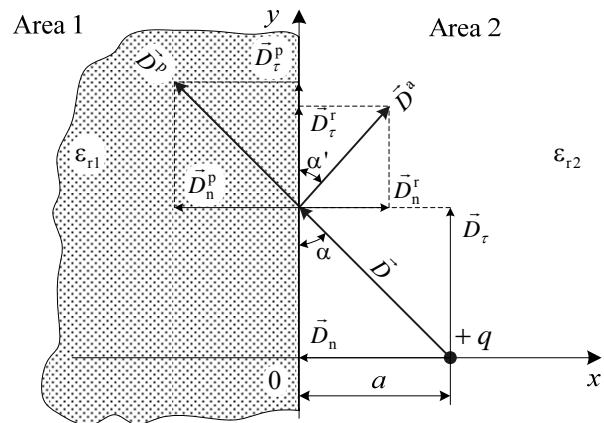


Fig. 2. Fluxes emanated by electric charge.

The principle of partial images [13] is applied to take into account the dielectric non-uniformity. Calculation of partial charge images and their position in MSL cross-section in the best way to show processes occurring on the flat interface of two infinite dielectric half-areas, having placed in one of them the linear charge  $+q$ . Such half-areas with relative permittivities  $\epsilon_{r1}$  and  $\epsilon_{r2}$  correspondently, are shown in Fig. 2. In the area 2 on distance  $a$  from dielectric interface the linear charge  $+q$ , which emanates uniform in axial direction electric flux density  $\vec{D}$ , is placed. This flux, falling aslope on interface between dielectrics, is split on two parts.  $\vec{D}^r$  part is reflected and remains in the area 2.  $\vec{D}^p$  part is penetrate into the area 1.

The magnitudes of penetration  $K^p$  and reflection  $K^r$  coefficients are expressed in the forms:

$$K^r = \frac{D^r}{D}, \quad K^p = \frac{D^p}{D}. \quad (1)$$

On dielectrics interface falling, reflected and penetrated fluxes should satisfy to boundary conditions, i.e. normal components of the electric flux density and tangential components of the electric field should be continuous on both sides of the interface. The condition of the continuity of normal components of the electric flux  $D_n^p = D_n - D_n^r$  in our case is written in this form:

$$D^p \sin \alpha = D \sin \alpha - D^r \sin \alpha'. \quad (2)$$

When we divide each term of the equation (2) by the magnitude  $D$  and take into account that the incidence  $\alpha$  and the reflected  $\alpha'$  angles are equal to each other we obtain the expression:

$$K^p = 1 - K^a. \quad (3)$$

The boundary condition for tangential components of the electric field intensity vector  $E_\tau^p = E_\tau + E_\tau^r$  is written in this manner:

$$\frac{D^p \cos \alpha'}{\varepsilon_0 \varepsilon_{r1}} = \frac{D \cos \alpha}{\varepsilon_0 \varepsilon_{r2}} + \frac{D^r \cos \alpha}{\varepsilon_0 \varepsilon_{r2}}. \quad (4)$$

Simplifying equation (4), having divided it on  $D$  and taking into account interrelation of penetration and reflection coefficients (3), we shall receive the equation which characterizes dependence of reflection coefficient from permittivities of the areas

$$K^r = -\frac{\varepsilon_{r1} - \varepsilon_{r2}}{\varepsilon_{r1} + \varepsilon_{r2}}. \quad (5)$$

We suppose that the area 1 in Fig.2 has the same electrophysical parameters as the dielectric substrate of the MSL (Fig. 1) and that the permittivity is  $\varepsilon_{r1} = \varepsilon_r > 1$ . The permittivity of the area 2 corresponds with the air and  $\varepsilon_{r2} = 1$ . Hence in the model of MSL the reflection coefficient calculated by such an equation:

$$K = K^a = -\frac{\varepsilon_r - 1}{\varepsilon_r + 1}. \quad (6)$$

It is much easier to replace various processes of penetration and reflection only with processes of penetration as it is shown in Fig. 3 (a). Here the reflected flux  $D^r$  is emanated by the partial image  $Kq$  of the charge  $+q$ . This image is placed in the area 1 at the point  $x = -a$  and is mirrored charge  $+q$  image from the interface between dielectrics (Fig. 3 (c)). The flux penetrated in the area 1 is emanated by the partial image  $(1-K)q$  which is situated in the area 2 on a place of charge  $+q$ ,  $x = a$  (Fig. 3 (b)). Thus, the electric flux density in the 1-st area is characterizes by the flux, which is emanated by the partial image  $(1-K)q$ , located in the area 2, and the reflected electric flux density in the area 2 characterizes the flux that is emanated by the partial image  $Kq$  which is situated in the area 1.

The partial charge images together with the original charge are applied to derivation of the Green functions which define the potential in the relevant area. For determination of the potential which raises due to partial charge image  $(1-K)q$ , in the area 1, shown in Fig. 3 (b), such Green function is applied:

$$G(P_j : P_i) = -\frac{1-K}{4\pi\varepsilon_r\varepsilon_0} \ln \left[ (x_j - a)^2 + (y_j - y_i)^2 \right] \quad (7)$$

and in the area 2 – raised by an original charge which is located in the point  $x = a$ , and the partial image, which is located in the point  $x = -a$  (Fig. 3 (b)), such Green function is applied:

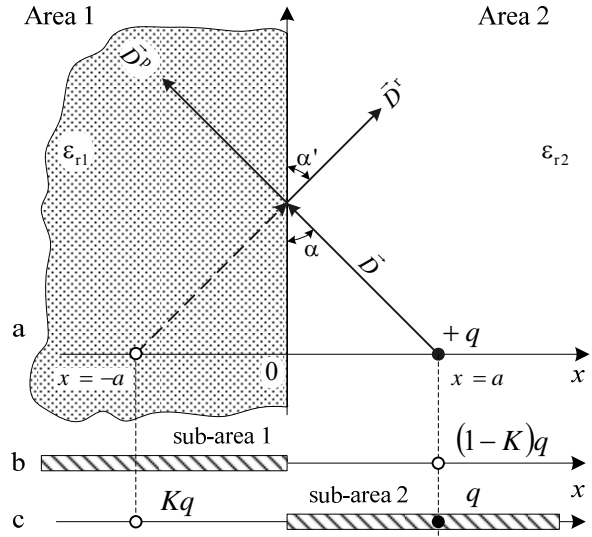


**Fig. 3.** Fluxes emanated from the electric charge and its partial images (a); sketches of the locations of the charge and the partial images in the dielectric media (b), and in the air (c).

$$G(P_j : P_i) = -\frac{1}{4\pi\varepsilon_0} \left\{ \ln \left[ (x_j - a)^2 + (y_j - y_i)^2 \right] + K \ln \left[ (x_j + a)^2 + (y_j - y_i)^2 \right] \right\}; \quad (8)$$

where  $G(P_j : P_i)$  is the Green function which defines the potential of point  $P_j \equiv (x_j, y_j)$  which is raised by a charge placed in point  $P_i \equiv (x_i, y_i)$ . So the principle of partial images allows us to find the electric potential at each point of the MSL knowing the charge, its partial image and the distance from each of them to any point which we analyze.

### Partial charge images in the dielectric substrate

In Fig. 4 the charges located close to the infinite dielectric layer (in the axis  $y$  direction) which has the thickness equal to  $2h$ . The thickness  $2h$  was chosen in order to eliminate the metal ground plane from our calculations by using the same electrodynamical principle of the mirror charge images. In this case, the Green function is derived for each of three areas, shown in this figure, separately. Generally, the number of images is infinite and each of them refers to as the partial image.

Due to the fact that the electric flux density was reflected from the dielectric surface inside the substrate and the part of it has penetrated into free space (see Fig. 4), the  $K$  calculated by equation (6), becomes positive (interchanging the position of  $\varepsilon_{r1}$  and  $\varepsilon_{r2}$  accordingly), keeping the same numerical value. Thus, lines of the flux which have penetrated in dielectric and have left it, in their equations contain such expressions of coefficients:

$$(1-K)(1+K) = (1-K^2).$$

Having made the diagram of partial images in the finite thickness dielectric substrate (Fig. 4), the Green function of each of three areas may be described using the potential function expressed by the infinite sequence:

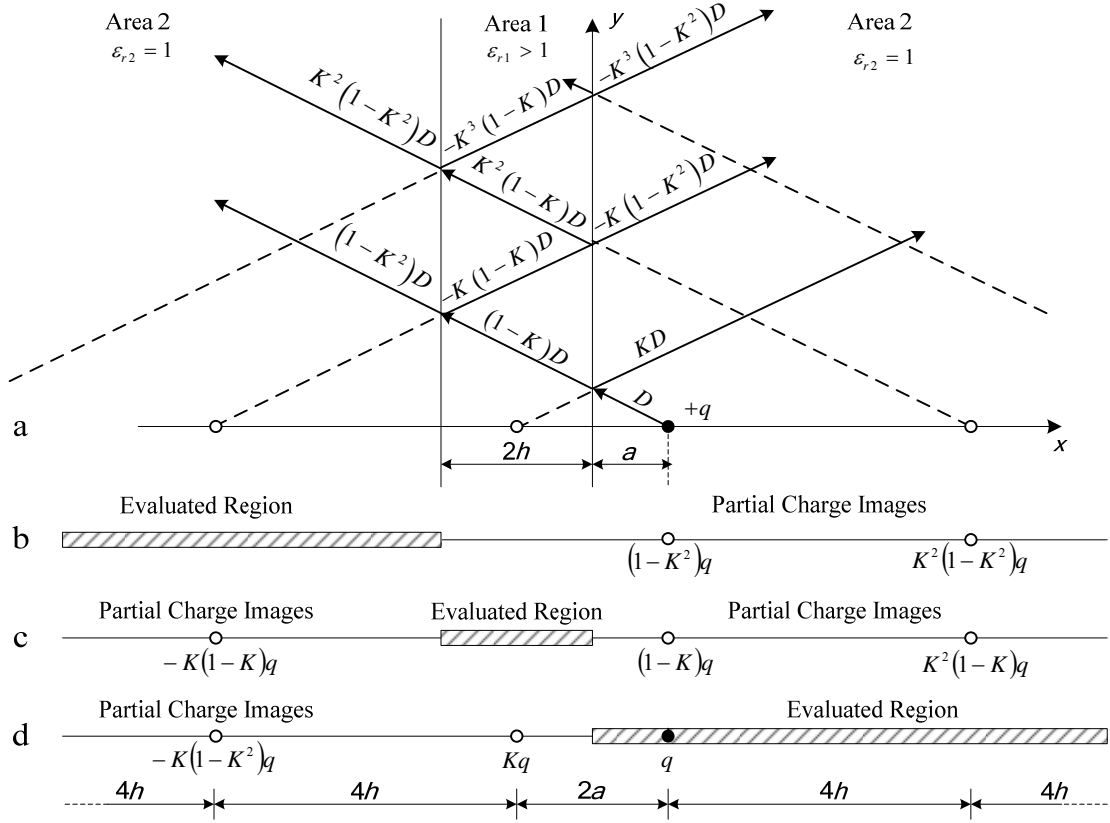


**Fig. 4.** The electric fluxes emanated by a charge and its partial images, in the area of a dielectric substrate (a); diagrams for definition of Green function in air half-area under the dielectric substrate (b); in the dielectric substrate (c); and in half-area above the substrate (d).

$$\varphi(P_j : P_i) = -\sum_{i=1}^{\infty} \frac{1}{4\pi\epsilon} q_i \times \times \ln \left[ (x_j - x_i)^2 + (y_j - y_i)^2 \right]; \quad (9)$$

where  $q_i$  is the charge corresponding the  $i$ -th image, or, in corresponding cases, the true charge situated in the  $P_i \equiv (x_i, y_i)$  point. In this equation  $\epsilon = \epsilon_r \epsilon_0$  or  $\epsilon = \epsilon_0$ , should correspond analyzed point  $P_j$ , instead of point  $P_i$  of location of the partial charge image.

### Mathematical model creation technique

Creating the model of the microstrip line, the strip we located in one of half-areas and divided on  $N$  partial sections. Charge density  $\rho_i$  of each partial section is unknown. For convenience, we shall consider, that in cross-section of infinitely long MSL charge density  $\rho_i$  concentrates in the point charge  $q_i = \rho_i \cdot \Delta W$  placed in the center of the  $i$ -th partial section, whose width is  $\Delta W = W/N$  (see Fig. 5). Ground plane in the model is done creating for each point charge its mirror image  $-q_i$ . It is seen in Figure 5, that charges in the model of the microstrip line have come nearer to a dielectric surface  $a \rightarrow 0$ . Hence, the potential of point  $P_j$  which raises by the charge which is situated in the same point, is calculated

as self-potential composing charge  $q_j$  and its first partial image  $Kq_j$  (see Fig. 4, (d)), i.e.  $q_j + Kq_j = (1+K)q_j$ .

Thus mathematical model of the microstrip line will consist of the system of the linear equations which describe dependence of potentials on charge densities  $\rho_i$ . As in the model there are two planes of symmetry, the system of equations will make only  $N/2$  independent equations.

Then applying the principal of images we can complete the process of finding out the influence of each charge on the electric potential at a certain point by using six steps:

1. The self-potential which is raised by the charge  $q_j$  situated in the same point and its first partial image  $Kq_j$  is determined

$$\varphi(P_j : P_j) = -\frac{(1+K)q_j}{2\pi\epsilon_0} \left[ \ln \left( \frac{\Delta W}{2} \right) - 1 \right]; \quad (10)$$

where  $\Delta W$  is the width of the partial section (see Fig. 5).

2. The potential which is raised by other partial images of the charge  $q_j$  is determined

$$\varphi(P_j : P_j) = \frac{K(1-K^2)q_j}{2\pi\epsilon_0} \sum_{n=1}^{\infty} K^{2(n-1)} \ln(4nh). \quad (11)$$

3. The potential which is raised by charge  $-q_j$  and all its partial images which are situated in point  $P_{N+j}$  is determined

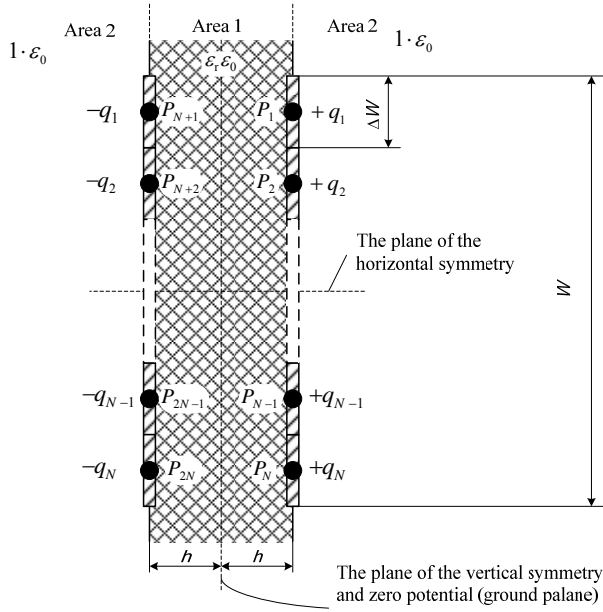


Fig. 5. Division of the microstrip line into partial sections.

$$\varphi(P_j : P_{N+j}) = \frac{(1-K^2)q_j}{2\pi\epsilon_0} \times \sum_{n=1}^{\infty} K^{2(n-1)} \ln[(4n-2)h]. \quad (12)$$

4. The potential which is raised by mirror charge  $q_j$  and its first partial image  $Kq_j$  which are in point  $P_{N-j+1}$  is determined

$$\varphi(P_j : P_{N-j+1}) = -\frac{(1+K)q_j}{2\pi\epsilon_0} \times \ln[(N-j+1)\Delta W]. \quad (13)$$

5. The potential which is raised by other partial images of the mirror charge  $q_j$  which are in point  $P_{N-j+1}$  is determined

$$\varphi(P_j : P_{N-j+1}) = \frac{K(1-K^2)q_j}{4\pi\epsilon_0} \times \sum_{n=1}^{\infty} K^{2(n-1)} \ln\left\{[(N-j+1)\Delta W]^2 + (4nh)^2\right\}. \quad (14)$$

6. The potential which is raised by charge  $-q_j$  and all its partial images which are situated in point  $P_{2N-j+1}$  is determined

$$\varphi(P_j : P_{2N-j+1}) = \frac{(1-K^2)q_j}{4\pi\epsilon_0} \sum_{n=1}^{\infty} K^{2(n-1)} \times \ln\left\{[(2N-j+1)\Delta W]^2 + [(2n-1)2h]^2\right\}. \quad (15)$$

If the potential in the point  $j$  raised by charge  $q_i$  which is in point  $i$  is determined, then expressions on the 1-st and 2-nd steps will be others. On the 1-st step:

$$\varphi(P_j : P_i) = -\frac{(1+K)q_i}{2\pi\epsilon_0} \ln(|j-i|\Delta W). \quad (16)$$

On the 2-nd step:

$$\varphi(P_j : P_i) = \frac{K(1-K^2)q_i}{4\pi\epsilon_0} \times \sum_{n=1}^{\infty} K^{2(n-1)} \ln\left\{[(i-j)\Delta W]^2 + (4nh)^2\right\}. \quad (17)$$

Having determined all components of potentials, the system of the linear equations describing potentials in points  $P_1 \dots P_{N/2}$  is made

$$\begin{cases} 1 = A_{11}q_1 + A_{12}q_2 + \dots + A_{1\frac{N}{2}}q_{\frac{N}{2}} \\ 1 = A_{21}q_1 + A_{22}q_2 + \dots + A_{2\frac{N}{2}}q_{\frac{N}{2}} \\ \dots \\ 1 = A_{\frac{N}{2}1}q_1 + A_{\frac{N}{2}2}q_2 + \dots + A_{\frac{N}{2}\frac{N}{2}}q_{\frac{N}{2}} \end{cases}. \quad (18)$$

Equation (18) in the matrix form looks so:

$$[1] = [A] \times [q]. \quad (19)$$

Coefficients  $A_{ij}$  of equation (18) characterize potential in point  $P_i$ , raised by charge  $q_j$ . In our case they are finding with the help of corresponding addition of the potentials determined according to expressions (9)–(16)

$$A_{ij} = \sum_{j=1}^6 \varphi(P_i : P_j). \quad (20)$$

The matrix-column of unknown charges  $[q]$  in equation (19) is finding solving of such an equation:

$$[q] = [A]^{-1} \times [1]. \quad (21)$$

The capacity per unit length of the microstrip line is determined by addition of capacities of all  $N$  partial areas.

$$C_1 = \frac{\sum_{i=1}^N q_i}{1}. \quad (22)$$

Then, the characteristic impedance of the microstrip line can be determined using such an expression [1]:

$$Z = \frac{1}{c_0 \sqrt{C_1 C_{01}}}; \quad (23)$$

where  $c_0$  is the light speed in free space;  $C_{01}$  is the capacity of the MSL per unit length when the dielectric substrate in it is replaced by the air.

## Results of investigation of the microstrip line model

For check of correctness of mathematical model the software, using (9)–(17) and (20)–(22) expressions have been developed, that allow to calculate the charge distribution in the strip of MSL cross-section, the capacity of MSL per length unit, and the characteristic impedance

**Table 1.** Characteristic impedance of microstrip lines with the various constructional parameters, calculated by various methods.

$W/h$	$\epsilon_r = 6.0$			$\epsilon_r = 9.6$			$\epsilon_r = 13.0$			$\epsilon_r = 28.0$		
	$Z, \Omega$	$Z_{[5]}, \Omega$	$Z_{[6]}, \Omega$	$Z, \Omega$	$Z_{[5]}, \Omega$	$Z_{[6]}, \Omega$	$Z, \Omega$	$Z_{[5]}, \Omega$	$Z_{[6]}, \Omega$	$Z, \Omega$	$Z_{[5]}, \Omega$	$Z_{[6]}, \Omega$
0,1	134,7143	134,72	134,78	109,0053	109,01	109,06	94,6657	94,670	94,718	65,5756	65,578	65,612
0,2	112,4978	112,50	112,58	90,948	90,952	91,020	78,9519	78,955	79,015	54,6559	54,658	54,699
0,4	90,3807	90,385	90,482	72,9718	72,975	73,054	63,3088	63,312	63,381	43,7853	43,787	43,835
0,7	72,7845	72,789	72,892	58,6731	58,676	58,761	50,8671	50,870	50,943	35,1407	35,143	35,194
1,0	61,8807	61,885	61,987	49,8175	49,821	49,904	43,1634	43,166	43,238	29,7903	29,792	29,843
2,0	42,2886	42,293	42,376	33,9308	33,934	34,001	29,3535	29,357	29,415	20,2099	20,212	20,249
4,0	26,4489	26,454	26,503	21,1389	21,143	21,183	18,2547	18,258	18,282	12,5332	12,536	12,555
10,0	12,7179	12,726	12,745	10,1186	10,125	10,140	8,7201	8,7260	8,7392	5,9678	5,9720	5,9808

of MSL. By suggested model the calculated values of the characteristic impedance of MSL at various ratios  $W/h$  and various permittivities of the dielectric substrate, are submitted in Table 1.

During calculations the strip of MSL has been divided into 750 partial sections. The amount of partial sections was selected consecutively increasing their number until the difference of the capacities per length unit of MSL there were no less than 0.001 %. Summation of infinite sequences of expressions (13), (14) and (16) were stopped when addition of the new member did not result in relative change of the sum less than 0.0001 %.

For comparison in Table 1 values of the characteristic impedance of MSL with the similar parameters, received by the method of integrated equations [5] and the spectral-domain method [6] are also submitted. Comparing these results it is easy to notice, that values of a characteristic impedance of the MSL, calculated according to offered mathematical model, are little bit less than the values received by other methods. However the relative difference with the method of integral equations does not exceed 0.07 %, and with a spectral-domain method – 0.22 %.

At the specified number of partial sections and limits of summation of sequences, calculations proceeded till 3 minutes (computer configuration: CPU – Pentium® IV 2.6 GHz, RAM – 512 MB, HDD – 80 GB). The increase in number of partial sections and length of summable sequences demands additional computer resources. Meanwhile, hardly having reduced requirements to accuracy of calculations concerning compared results, computer resources are considerably released and calculations are accelerated. For example, having increased the relative difference with the integral equations method and the spectral-domain method up to 1 %, the number of partial sections in the offered mathematical model can be reduced up to 30, and calculations proceed approximately only 0.5 s.

For an illustration of dielectric non-uniformity in Figures 6 and 7 the normalized distributions of charges in cross-section of the signal strip are shown, at various design parameters of MSL.

It is seen in Figure 6, that dielectric non-uniformity practically does not change character of dependence of the charge distribution in given width strip cross-section of MSL. Installation of the dielectric substrate in the construction of the strip transmission line having the uniform dielectric ( $\epsilon_r = 1.0$ ), accordingly increases charges in all partial sections of the strip cross-section.

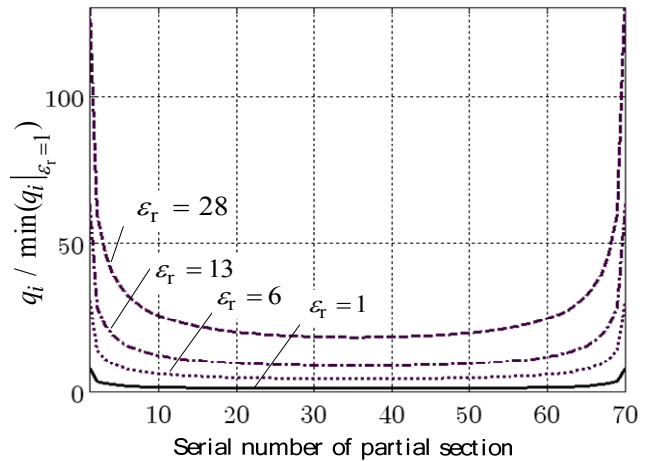


**Fig. 6.** The normalized distribution of the charge in cross-section of the strip of MSL at various values of dielectric permittivity, when  $W/h = 1, 0$ .

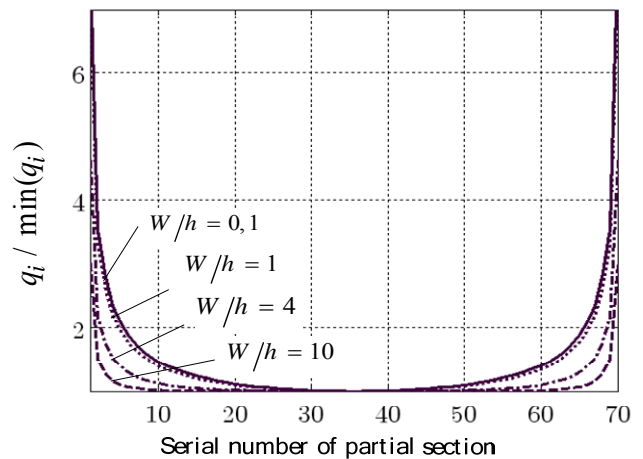


**Fig. 7.** The normalized distribution of the charge in cross-section of the strip of MSL at various values strip width, when  $\epsilon_r = 9, 6$ .

Dependences of charge distribution in cross-section of MSL strip at various ratio of its width and thickness of dielectric substrate  $W/h$  are submitted in Figure 7. It may be noted, that in narrow strips or in lines with thicker dielectric substrate, the edge effect of the electric field intensity is expressed more appreciably. The influence on such changes renders non-uniformity of the dielectric of analyzed MSL and the sizes of its cross-section.

## Conclusions

1. Taking into account continuous increase of computer resources and perfection of the software, for increase of accuracy of the analysis of microstrip lines it is expedient to apply analytically more simple numerical methods.

2. The characteristic impedance of the microstrip line and some other its parameters can be calculated knowing charge distribution in its cross-section at quasi-static approach.

3. Usual use of method of the moments allows to find electric charge distribution in cross-section of the transmission strip line with uniform dielectric.

4. Using the method of the moments and hte principle of partial images, the mathematical model of the microstrip line is developed. The model allows to find the electric charge distribution in strip cross-section of the microstrip line, and also to calculate its capacity per length unit and the characteristic impedance, at any ratio of width of the strip and thickness of the dielectric substrate, and also at any combinations of dielectrics of the substrate and environment above the substrate. The developed model demonstrates high accuracy and significant speed.

## References

1. **Gupta K. C., Garg R., Bahl I.** Microstrip Lines and Slotlines (Artech House Microwave Library) / Artech House. 1996. 535 p.
2. **Wadell B.C.** Transmission Line Design Handbook (Artech House Microwave Library) / Artech House. 1991. 500 p.
3. **Штарас С., Станкунас Й.** Частотные свойства спиральных отклоняющих систем // Техника средств связи: Радиоизмерительная техника, 1985. – Вып. 3. – С. 79–95.

**V. Urbanavičius, R. Martavičius. Model of the Microstrip Line with a Non-uniform Dielectric // Electronics and Electrical Engineering. – Kaunas: Technologija, 2006. – No. 3(67). – P. 55–60.**

The mathematical model of the microstrip line (MSL) with non-uniform dielectric in its cross-section is represented in the article. Supposed mathematical model is created using the method of moments and the technique of partial images of the charges. The created model allowed us to determine the charge distribution on the signal conductor, capacitance per unit length, and characteristic impedance of the MSL. The accuracy of supposed model was verified using the software which was created by authors. In this article the authors investigated electrodynamic characteristics of MSLs when it sizes and the substrate permittivity were changed in a wide range. A comparison of the calculated characteristics of author's model with the results from other articles showed that they coincided. Ill. 7, bibl. 13 (in English; summaries in English, Russian and Lithuanian).

**V. Урбанавичюс, Р. Мартавичюс. Модель микрополосковой линии учитывающей неоднородность диэлектрика // Электроника и электротехника. – Каунас: Технология, 2006. – № 3(67). – P. 55–60.**

Представлена математическая модель микрополосковой линии (МЛ) учитывающая неоднородность диэлектрика в поперечном сечении линии. Для построения математической модели использован метод моментов и принцип частичных отражений зарядов. Созданная модель позволяет установить распределение заряда на сигнальном проводнике линии, а также рассчитать погонную ёмкость и характеристический импеданс анализируемой МЛ. Точность созданной математической модели проверялась авторами с помощью написанного ими программного обеспечения. Были рассчитаны электродинамические параметры МЛ в широком интервале изменения конструктивных параметров линии. Проведённые расчёты показали хорошее совпадение получаемых результатов с публикуемыми в научной литературе. Ил. 7, библи. 13 (на английском языке; рефераты на английском, русском и литовском яз.).

**V. Urbanavičius, R. Martavičius. Mikrojuostelinės linijos modelis dielektriko nevienalytiškumui nustatyti // Elektronika ir elektrotechnika. – Kaunas: Technologija, 2006. – Nr. 3(67). – P. 55–60.**

Pateiktas mikrojuostelinės perdavimo linijos matematinis modelis, įvertinantis dielektriko nevienalytiškumą linijos skerspjūvyje. Matematiniam modeliui sudaryti pritaikytas momentų metodas ir krūvių dalinių atvaizdų principas. Sukurtas matematinis modelis leidžia nustatyti elektros krūvio pasiskirstymą signalinio laidininko skerspjūvyje, taip pat apskaičiuoti analizuojamos mikrojuostelinės linijos ilginę talpą ir būdingąjį impedansą. Siūlomo modelio tikslumas patikrintas autorių sukurta programine įranga. Skaičiavimai rezultatai gerai sutampa su publikuotais mokslinėje spaudoje, esant plačiam analizuojamų mikrojuostelinių linijų konstrukcinių parametrų ruožui. Il. 7, bibl. 13 (anglų kalba; santraukos anglų, rusų ir lietuvių k.).

4. **Martavičius R., Urbanavičius V.** Meandrinių lėtinimo sistemų banginė varža // Elektronika ir elektrotechnika. – Kaunas: Technologija, 1997. – Nr. 1(10). – P. 14–16.
5. **Homentcoschi D.** High Accuracy Formulas for Calculation of the Characteristic Impedance of Microstrip Lines // IEEE Trans. on Microwave Theory and Techniques, 1995, vol, MTT-43, No. 9. – P. 2132–2137.
6. **Cheng K.K.K., Everard K.A.** Accurate Formulas for Efficient Calculation of the Characteristic Impedance of Microstrip Lines // IEEE Trans. on Microwave Theory and Techniques, 1991, vol, MTT-39, No. 9. – P. 1658–1661.
7. **Kleiza A., Štaras S.** Daugialaidžių linijų banginių varžų skaičiavimas // Elektronika ir elektrotechnika. – Kaunas: Technologija, 1999 – Nr. 4 (22). – P. 41–44.
8. **Martavičius R., Urbanavičius V.** Metodika nepastovaus žingsnio daugialaidės linijos ilginėms talpoms apskaičiuoti // Elektronika ir elektrotechnika. – Kaunas: Technologija, 2002. – Nr. 6 (41). – P. 47–53.
9. **Skudutis J., Daškevičius V., Garšva E.** Microwave Office programų paketo taikymo lėtinimo sistemų tyrimui patirtis // Elektronika ir elektrotechnika. – Kaunas: Technologija, 2004. – Nr. 2 (51) – P. 68–73.
10. **Turker N., Gunez F.** An Artificial Neural Model of the Microstrip Lines // Signal Processing and Communications Applications Conference, 2004. Proceedings of the IEEE 12th. – P. 657–660.
11. **Harrington R. F.** Field Computation by Moment Methods / IEEE Press, New York, 1993. 229 p.
12. **Sadiku M. N. O.** Numerical Techniques in Electromagnetics/ CRC Press. 2001. 760 p.
13. **Silvester P. P., Ferrari R. L.** Finite Elements for Electrical Engineers/ Cambridge, UK: Cambridge University Press. 1996. 512 p.

Presented for publication 2006 01 18